Details on discrete time case

In this section we illustrate the derivation of the numerical implementation of our proposed method based on the BBK integrator. We calculate the RE estimators based on the derived state transition probabilities.

Calculation of transition probabilities

After reordering the equations of the BBK integrator we get (matrix form) the expressions for the new timestep $i+1$

$$\begin{cases} \boldsymbol{q}_{i+1} = \boldsymbol{q}_i + M^{-1}\Delta t(I - \gamma M^{-1}\frac{\Delta t}{2})\boldsymbol{p}_i - M^{-1}\frac{\Delta t^2}{2}\nabla V(\boldsymbol{q}_i) + M^{-1}\Delta t\sqrt{2\gamma\beta^{-1}}\Delta W_i \\ (I + \gamma M^{-1}\frac{\Delta t}{2})\boldsymbol{p}_{i+1} = (\frac{M}{\Delta t})\Delta \boldsymbol{q}_i - \nabla(V(\boldsymbol{q}_{i+1}))\frac{\Delta t}{2} + \sqrt{2\gamma\beta^{-1}}\Delta W_{i+\frac{1}{2}} \end{cases} \tag{1}$$

From the above set of normal distributions we define the transition probability as a product of two independent normal ones:

$$P(\boldsymbol{q}_i, \boldsymbol{p}_i \to \boldsymbol{q}_{i+1}, \boldsymbol{p}_{i+1}) = P(\boldsymbol{q}_{i+1}|\boldsymbol{q}_i, \boldsymbol{p}_i)P(\boldsymbol{p}_{i+1}|\boldsymbol{q}_i, \boldsymbol{p}_i, \boldsymbol{q}_{i+1}) \tag{2}$$

This splitting of P is feasible because the numerical scheme of BBK is non-degenerate. The corresponding formulas after reordering eq. (1) are:

$$P(\boldsymbol{q}_{i+1}|\boldsymbol{p}_i, \boldsymbol{q}_i) = \frac{1}{((2\pi)^{dN} det(\Delta t^3\gamma\beta^{-1}M^{-2}))^{1/2}} \times \exp\Big\{ - \frac{\beta}{2\Delta t^3\gamma} \\ ||\Delta \boldsymbol{q}_i - M^{-1}\Delta t(I - \frac{\gamma\Delta t M^{-1}}{2})\boldsymbol{p}_i + M^{-1}\frac{\Delta t^2}{2}\nabla V(\boldsymbol{q}_i)||^2_{M^2}\Big\}$$

$$P(\boldsymbol{p}_{i+1}|\boldsymbol{p}_i, \boldsymbol{q}_i, \boldsymbol{q}_{i+1}) = \frac{1}{((2\pi)^{dN} det(\Delta t\gamma\beta^{-1}Id)^{1/2}} \times \exp\Big\{ - \frac{\beta}{2\Delta t\gamma} \\ ||(I + \frac{\gamma\Delta t M^{-1}}{2})\boldsymbol{p}_{i+1} - \frac{M}{\Delta t}\Delta \boldsymbol{q}_i + \nabla V(\boldsymbol{q}_{i+1})\frac{\Delta t}{2}||^2\Big\}$$

where

$$||x||_M = x^T M x, \quad M \in \mathbb{R}^{dN\times dN}, x \in \mathbb{R}^{dN}$$

$$M^{-1} = diag\Big(\underbrace{\frac{1}{m_1}, \dots, \frac{1}{m_1}}_{\text{d-times}}, \dots, \frac{1}{m_N}\Big)$$

hence

$$det\Big(\Delta t^3\gamma\beta^{-1}M^{-2}\Big) = \Big(\Delta t^3\gamma\beta^{-1}\Big)^{dN}\prod_{i=1}^{N} m_i^{-2d}$$

Detailed Calculation of RER and path-wise FIM for BBK

The statistical estimator $\bar{H}_1$ (obtained from the Radon-Nikodym derivative) is utilized (see Ref. [1] in main text)

$$\bar{H_1}^{(n)} = \frac{1}{n\Delta t}\sum_{i=0}^{n-1} \log \frac{P^{\theta}(\boldsymbol{z}_i, \boldsymbol{z}_{i+1})}{P^{\theta+\epsilon_0}(\boldsymbol{z}_i, \boldsymbol{z}_{i+1})} \tag{3}$$

The corresponding estimator for FIM derived in the same fashion is:

$$\bar{F_1}^{(n)} = \frac{1}{n\Delta t}\sum_{i=0}^{n-1} \nabla_{\theta} \log P^{\theta}(\boldsymbol{z}_i, \boldsymbol{z}_{i+1}) \nabla_{\theta} \log P^{\theta}(\boldsymbol{z}_i, \boldsymbol{z}_{i+1})^T \tag{4}$$

From eq.'s (2) and (3) the RER is given by:

$$\begin{aligned} \bar{H}_1(\bar{Q}^{\theta}|\bar{Q}^{\theta+\epsilon_0}) &= \frac{1}{n\Delta t}\sum_{i=0}^{n-1} log \frac{P^{\theta}(\boldsymbol{q}_i, \boldsymbol{p}_i \to \boldsymbol{q}_{i+1}, \boldsymbol{p}_{i+1})}{P^{\theta+\epsilon_0}(\boldsymbol{q}_i, \boldsymbol{p}_i \to \boldsymbol{q}_{i+1}, \boldsymbol{p}_{i+1})} \\ &= \frac{1}{n\Delta t}\sum_{i=0}^{n-1} \Big[log \frac{P^{\theta}(\boldsymbol{q}_{i+1}|\boldsymbol{q}_i, \boldsymbol{p}_i)}{P^{\theta+\epsilon_0}(\boldsymbol{q}_{i+1}|\boldsymbol{q}_i, \boldsymbol{p}_i)} \\ &+ log \frac{P^{\theta}(\boldsymbol{p}_{i+1}|\boldsymbol{q}_i, \boldsymbol{p}_i, \boldsymbol{q}_{i+1})}{P^{\theta+\epsilon_0}(\boldsymbol{p}_{i+1}|\boldsymbol{q}_i, \boldsymbol{p}_i, \boldsymbol{q}_{i+1})} \Big] \end{aligned} \tag{5}$$

where

$$\log P^{\theta}(\boldsymbol{q}_{i+1}|\boldsymbol{p}_i, \boldsymbol{q}_i) = -\frac{1}{2}\log((2\pi)^{dN}(\Delta t^3 \gamma \beta^{-1})^{dN} \prod_{j=1}^{N} m_j^{2d})$$
$$- \frac{\beta}{2\Delta t^3 \gamma}\sum_{j=1}^{dN} m_j^2 \Big[(\Delta \boldsymbol{q}_i)_j - \frac{\Delta t}{m_j}(1 - \frac{\gamma \Delta t}{2m_j})(\boldsymbol{p}_i)_j + \frac{\Delta t^2}{2m_j}(\nabla_j V^{\theta}(\boldsymbol{q}_i)) \Big]^2$$

$$\log P^{\theta}(\boldsymbol{p}_{i+1}|\boldsymbol{p}_i, \boldsymbol{q}_i, \boldsymbol{q}_{i+1}) = -\frac{dN}{2}\log((2\pi \Delta t \gamma \beta^{-1})$$
$$- \frac{\beta}{2\gamma \Delta t}\sum_{j=1}^{dN} \Big[(1 + \frac{\gamma \Delta t}{2m_j})(\boldsymbol{p}_{i+1})_j - \frac{m_j}{\Delta t}(\Delta \boldsymbol{q}_i)_j + \frac{\Delta t}{2}(\nabla_j V^{\theta}(\boldsymbol{q}_{i+1})) \Big]^2$$
$$, \quad (\Delta \boldsymbol{q}_i)_j = (\boldsymbol{q}_{i+1})_j - (\boldsymbol{q}_i)_j, \quad \nabla_j = \frac{\partial}{\partial q_j}$$

$(\Delta \boldsymbol{q}_i)_j$ is the momentum difference of atom j in time. The Fisher information matrix (FIM) is $k \times k$ in dimension, (for the CH_4 model studied here k = 10, which include the LJ $\epsilon_{LJ}, \sigma_{LJ}$, bond and angle coefficients) and the (l,m)-th element at the i-th timestep is given by the partial derivatives of (2) with respect to the potential coefficients:

$$
\begin{aligned}
&(\nabla_\theta \log P^\theta(\boldsymbol{z}_i, \boldsymbol{z}_{i+1}) \nabla_\theta \log P^\theta(\boldsymbol{z}_i, \boldsymbol{z}_{i+1})^T)_{l,m} = \\
&\Big[\frac{\partial}{\partial \theta_l}(\log P^\theta(\boldsymbol{q}_{i+1}|\boldsymbol{q}_i, \boldsymbol{p}_i)) + \frac{\partial}{\partial \theta_l}(\log P^\theta(\boldsymbol{p}_{i+1}|\boldsymbol{q}_i, \boldsymbol{p}_i, \boldsymbol{q}_{i+1}))\Big] \times \\
&\Big[\frac{\partial}{\partial \theta_m}(\log P^\theta(\boldsymbol{q}_{i+1}|\boldsymbol{q}_i, \boldsymbol{p}_i)) + \frac{\partial}{\partial \theta_m}(\log P^\theta(\boldsymbol{p}_{i+1}|\boldsymbol{q}_i, \boldsymbol{p}_i, \boldsymbol{q}_{i+1}))\Big]
\end{aligned} \tag{6}
$$

where

$$
\begin{aligned}
&\frac{\partial}{\partial \theta_m}(\log P^\theta(\boldsymbol{q}_{i+1}|\boldsymbol{q}_i, \boldsymbol{p}_i)) = \\
&\quad - \frac{1}{\sigma^2 \Delta t} \sum_{j=1}^{dN} m_j \Big[(\Delta \boldsymbol{q}_i)_j - \frac{\Delta t}{m_j}(1 - \frac{\Delta t \gamma}{2m_j})(\boldsymbol{p}_i)_j + \frac{\Delta t^2}{2m_j}(\nabla_j V^\theta(\boldsymbol{q}_i))\Big] \\
&\quad \times \frac{\partial}{\partial \theta_m}(\nabla_j V^\theta(\boldsymbol{q}_i)) \\
&\frac{\partial}{\partial \theta_m}(\log P^\theta(\boldsymbol{p}_{i+1}|\boldsymbol{q}_i, \boldsymbol{p}_i, \boldsymbol{q}_{i+1})) = \\
&\quad - \frac{1}{\sigma^2} \sum_{j=1}^{dN} \Big[(1 + \frac{\gamma \Delta t}{2m_j})(\boldsymbol{p}_{i+1})_j - \frac{m_j}{\Delta t}(\Delta \boldsymbol{q}_i)_j + \frac{\Delta t}{2}(\nabla_j V^\theta(\boldsymbol{q}_{i+1}))\Big] \\
&\quad \times \frac{\partial}{\partial \theta_m} \nabla_j V^\theta(\boldsymbol{q}_{i+1})
\end{aligned}
$$

RER and FIM calculations for the LJ fluid are summarized in Figure 1. We compare the RER value using the discrete time estimators (3), (4) and the middle bar corresponds to the FIM-based RER (eq.(5) in paper, when $T \to \infty$) whereas the left and right bars are the values of estimator (3) for a negative and positive perturbation by $\epsilon_0 = 5\%$ respectively. The perturbation in the figures is in logscale. The errorbars (variance) of the RER estimator is larger than the one corresponding to FIM, necessitating more samples for accurate estimation. All the plots are normalized upon division with the number of particles and simulations of bigger systems under the same parameters produce the same results. As the figure suggests σ_{LJ} is the most sensitive parameter.

We conclude that the discrete time version is in very good agreement, $O(\Delta t)$, with the continuous time version in the main text.

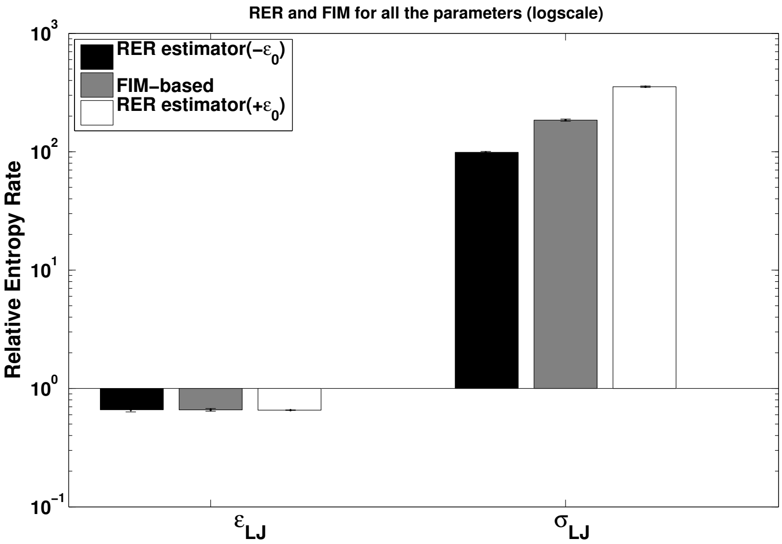

Figure 1: FIM based RER (per particle) for various directions using the two different estimators (3), (4). LJ parameters perturbed by $\pm 5\%$. The plot is in logscale and the most sensitive variable is σ_{LJ} (the errorbars are indecipherable). The variance of the RER estimator is larger than the one corresponding to FIM thus more samples are needed.